THE SnO_2 NANOTUBE WITH CNT CORE STRUCTURE (SnO_2@VOID@CNT) AND GRAPHENE COMPOSITE ELECTRODE FOR LI-ION BATTERIES

by

Mirac ALAF*

Department of Metallurgical and Materials Engineering, Bilecik Seyh Edebali University, Bilecik, Turkey

Original scientific paper
https://doi.org/10.2298/TSCI2304217A

In this study, the problem of volume expansion and agglomeration of SnO_2-based electrode materials has been solved with a unique and multifaced approach. Nanosized SnO_2 is coated around CNT with a void and this structure is decorated between graphene sheets. The problem of aggregation and volume expansion has been solved with nanostructure and voided structure. Besides, conductivity and buffering contributions have been provided by the production composite with graphene and CNT. Herein graphene layers were decorated SnO_2 nanotube with CNT core structure (SnO_2@void@CNT) and used as an anode for Li-ion battery. The electrodes were produced by vacuum filtration technique as flexible and free-standing with no any binder. To compare, pure SnO_2 and SnO_2 decorated graphene/CNT skeleton anodes were prepared and characterized. The SnO_2@void@CNT/graphene anode exhibited excellent cycling performance and rate capability properties.

Key words: *tin oxide, CNT, graphene, anode, Li-ion battery*

Introduction

The growing global energy demand of the modern world pushes towards more environmentally friendly and more renewable large-scale energy sources in contrast to fossil fuels such as oil, coal and natural gas [1]. The increase in CO_2 emissions and the limited amount of oil also necessitate finding clean energy sources. In this context, electrochemical systems used for energy generation, conversion and storage, including batteries, supercapacitors and fuel cells, play an important role [2]. It is known that especially rechargeable lithium batteries will play a key role in future energy storage systems, including portable electronic circuits (computer, smart phone, *etc.*) and automotive (electric or hybrid vehicles) applications [3]. The Li-ion batteries have a unique combination of high energy and power density. This feature makes Li-ion batteries a preferred technology for portable electronic circuits, power tools, and electric or hybrid vehicles [4]. Li-ion batteries will significantly reduce CO_2 emissions when electric vehicles replace petrol-powered vehicles. The high energy efficiency of Li-ion batteries enables these batteries to be used in electricity transmission applications used to improve the quality of energy obtained from wind, solar, geothermal and other RES. That is why Li-ion batteries are interesting for both industry and academic studies [5-7].

* Author's, e-mail: mirac.alaf@bilecik.edu.tr

Among the electrode materials for Li-ion batteries, tin oxide (SnO_2) is the most promising due to its low cost, environmental friendliness, high theoric specific capacity (1491 mAh/g), high columbic efficiency, good cycling ability and low operating voltage [8-10]. However, there are some obstacles to the commercial use of SnO_2-based electrode materials: large initial irreversible loss of capacity due to the formation of a thick solid electrolyte interphase during the cycle, volume changes during the charge/discharge process causing pulverization, and small active Sn particles aggregate into larger, inactive Sn clusters during cycling [11-13]. The strategies necessary to solve these existing problems can be grouped under three main headings. Synthesizing various nanostructured tin oxide materials such as SnO_2 nanoparticles, nanowires, and nanospheres can be considered as the first solution proposal [14]. Nanoscale materials provide not only shorter diffusion distances for electrons and ions, but also a buffering effect on volume expansion [15]. Secondly, porous or hollow SnO_2 can be produced. This structure provides sufficient free space to avoid the pulverization problem and can support large volume changes [16]. However, when nanostructured or porous materials tend to aggregate during the cycle, it may not be a perfect solution on its own, especially for long cycles and high speeds. The third effective way to increase the capacity and cycle stability of SnO_2 is to embed SnO_2 into carbon-based materials to form composites [17, 18]. On the one hand, carbon-based materials (CNT, graphene, and amorphous carbon, *etc.*) also significantly increase the conductivity of the electrode. On the other hand, they also act as a buffer to prevent large volume expansion [6].

In this study, versatile solutions have been provided to the difficulties that SnO_2 suffers from as an anode material. The SnO_2 nanoparticles were deposited on the CNT surface by leaving a void space owing to the sacrificial SiO_2, and the SnO_2 nanotube with CNT core structure was obtained. Then, this structure was decorated by compressing it between graphene sheets produced by the Hummer method. The electrode was prepared as flexible and free-standing by vacuum filtration method.

Experimental section

Preparation of SnO_2@void@CNT/graphene composite electrode consists of two separate preliminary stages. First stage is production of graphene oxide from flake graphite by modified Hummer method which is explained and detailed in the Electronic Supplementary Information [19, 20]. Second stage is synthesis of SnO_2@void@CNT structure. Then, graphene oxide and SnO_2@void@CNT are combined together and the electrodes are produced by vacuum filtration as a free-standing and flexible. The production process is shown schematically in the fig. 1.

A typical producing process of SnO_2@void@CNT was as follows: MWCNT (from Array Nano) were oxidized within a mixed H_2SO_4/HNO_3 (3:1 by volume) to activation of the surfaces. The SiO_2 coating of CNT surfaces was carried out by hydrolysis of tetraethyl orthosilicate (TEOS) and polycondensation of SiO_2 reactions in compliance with the Stober method. The 100 mg oxidized MWCNT was dispersed in a mixed solution of 150 ml deionized water and ethanol with an ultrasonic processor for 0.5 hours. The CTAB was added as a surfactant to provide better dispersion and avoid agglomeration of CNT. After ultrasonication, the solution was taken on a magnetic stirrer and approximate 1.5 mL ammonia solution was added until arranged pH range to 10-12 and stirred for another 0.5 hours. Then, TEOS (1.5 mL) and ethanol (15 mL) were mixed in a separate beaker. The TEOS solution was added to this solution dropwise in one hour and was stirred for six hours at room temperature to complete the formation of silica coating. After the process, SiO_2@CNT was collected by vacuum

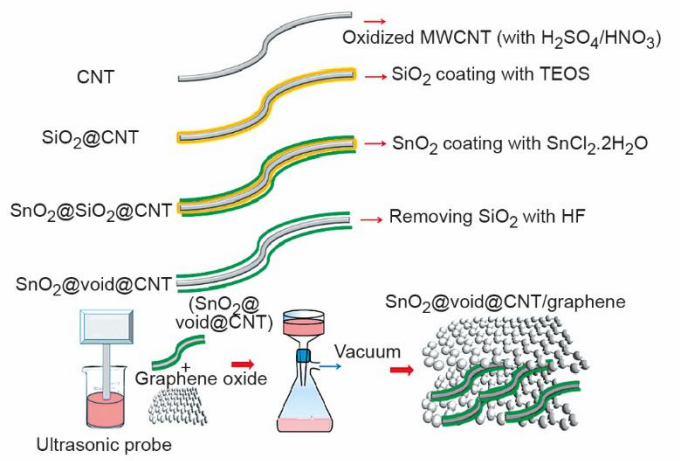

Figure 1. Schematic illustration of production and structure of SnO_2@void@CNT/graphene composite electrode

filtration, washed with ethanol and water and dried at 80 °C for 12 hours. The SnO_2@SiO_2@CNT was fabricated by a facile solvothermal method. Typically, 100 mg of SiO_2@CNT and CTAB were dispersed in 100 mL distilled water and ultrasonically treated for 30 minutes and 0.112 g of $SnCl_4$, 0.30 g of urea, acidic acid were added to the solution under magnetic stirring for one hour. The final product was obtained by vacuum filtration by washing with water several times. After being dried at 80 °C for 12 hours, SnO_2@SiO_2@CNT was obtained. Subsequently, SnO_2@SiO_2@CNT was selectively etched in 3% HF solution for 15 minutes to discard sacrificial SiO_2 layer to fabricate SnO_2@void@CNT structure. The etching process was performed slowly and precisely at a relatively low HF concentration. The obtained product was washed with water several times until a pH value of 6 was achieved and dried at 80 °C for 12 hours.

In order to prepare SnO_2@void@CNT/graphene composite electrode, graphene oxide, SnO_2@void@CNT structure and CTAB were co-dispersed in 100 mL de-ionized water for 30 minutes. The 5 mL hydrazine hydrate solution was directly added to reduce graphene oxide to graphene and sonication was carried on for an additional 15 minutes. The mixture was then vacuum filtered using PTFE filter paper (Millipore) with the pore size of 220 nm. Finally, the obtained free standing and flexible SnO_2@void@CNT/graphene electrode was dried at 80 °C and peeled off from filter paper. Since the filter paper had a diameter of 47 mm, the produced electrodes had to be cut into diameters suitable for the CR2016 cell. To make this more practical, a mold with the electrode diameter holes was placed on the filter paper and 3 electrodes could be produced at once. For compare, two more anodes were prepared as SnO_2 and SnO_2/CNT/graphene composite. Pure SnO_2 was synthesized with using $SnCl_4$ and SnO_2 anode was produced with the conventional slurry method. To produce free-standing and flexible SnO_2/CNT/graphene composite anode, pure SnO_2 powders were decorated CNT and graphene skeleton system by using the ultrasonic process and vacuum filtered through filter paper. Details of the preparing processes for these two electrodes are presented in the Electronic Supplementary Information

The X-ray diffraction patterns of the samples were recorded on a RIGAKU D/MAX 2000 X-ray diffractometer with Cu Kα radiation during a scan range of 5°-90° at a scan rate of 10° per minute. The morphologies of the samples were observed by a SEM (FEG SEM,

JEOL 6335F) transmission electron microscopy (TEM, Jeol JEM2100F). The thermogravimetric analysis was conducted using a thermal gravimetric analyzer (a NETZSCH DTA-TG, heating rate: 10 °C per minute, atmosphere: air) to determine weights of SnO_2 and carbon in composite anode.

Electrochemical properties were evaluated by using CR2016 half cells assembled in argon filled glove box. In the half cells, the free standing and flexible electrode, Li foil, a polypropylene (PP) film (Cellgard 2300) and 1 M lithium hexafluorophosphate ($LiPF_6$) solution in EC:DMC (1:1 by vol) were used as anode, cathode, separator and electrolyte, respectively. Charge-discharge tests were carried on a MTI BST8-MA Battery Analyzer with the potential range of 0.01-2.5 V at a constant current density of 200 mA/g. Cyclic voltammetry (0.01-3 V) was detected on a Gamry Instrument Version 5.67 at 0.2 mV/s. Electrochemical impedance spectroscopy (EIS) measurements were conducted on the same work station with the frequency range of 100 kHz-0.01 Hz.

Results

To produce SnO_2 nanotube with CNT core structure (SnO_2@void@CNT), the first stage is SiO_2 coating of CNT surface. Figure 2(a) shows an SEM image of SiO_2@CNT and we can see that CNT surfaces were smoothly coated with SiO_2 by hydrolysis of TEOS. For comparison, SEM image of acid-treated pure CNT is presented in fig. S1 and change of CNT before and after coating is clearly seen [21]. Second step is depositing SnO_2 crystals onto SiO_2@CNT structure. When coated with SnO_2, the smoothness of the SiO_2@CNT surface is disappeared and the diameter of the tubes is increased as can be seen in fig. 2(b). Last step is slight and slow etching of SnO_2@SiO_2@CNT structure with 3% HF solution. Figure 2(c) shows SnO_2@void@CNT structure after etching and removing SiO_2. The TEM analysis was used for further confirmation and detailed visual information of the structure, fig. 2(d). Having a void between the tube and SnO_2 and placing this structure between graphene layers have been provided to the volume expansion problems of SnO_2 during the cycling. Similar to the advantages of yolk-shell morphology, SnO_2@void@CNT/graphene composite can provide the adequate free space for alleviating the volume variation and accommodating the stress during lithiation.

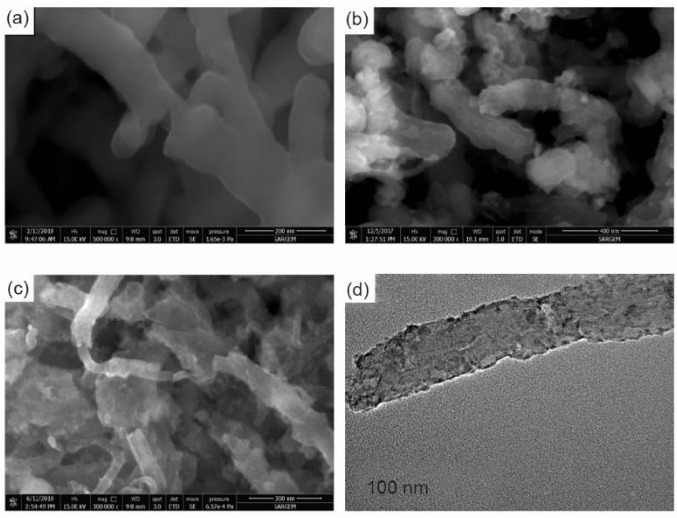

Figure 2. The SEM image of (a) SiO_2@CNT, (b) SiO_2@SnO_2@CNT, (c) SnO_2@void@CNT, (d) TEM image of SnO_2@void@CNT

During electrode production process, XRD analysis was employed to the samples after for each of the three steps. In addition, XRD results for pure SnO_2, bare CNT, graphite and graphene oxide are also given in the figs. S1- S4. Figure 3 presents XRD patterns of SiO_2@CNT, SnO_2@SiO_2@CNT and SnO_2@void@CNT/graphene composite electrodes. Considering of patterns of SiO_2@CNT (line 1) in fig. 3, it can be seen that a sharp diffraction peak is located at 26° which can be well indexed to CNT (JCPDS No. 00-026-1076) [22, 23]. Additionally, there is a broad diffraction peak located at around 20° indicating that amorphous SiO_2 phase [24, 25]. After SnO_2 depositing of SiO_2@CNT, the XRD pattern is seen as a line 2. Besides the CNT and amorphous SiO_2 peaks, the characteristic peaks of SnO_2 (JCPDS No.00-041-1445) are also clearly seen in the XRD pattern of SnO_2@SiO_2@CNT. It should be noted that the main peak of SnO_2 at 26° overlapped with the peak of CNT at 26° [26]. The SnO_2@void@CNT structure obtained after etching process of SnO_2@SiO_2@CNT was combined with graphene and electrodes were prepared by vacuum filtration. The upper pattern (line 3) shows SnO_2@void@CNT/ /graphene composite structure and contains SnO_2, CNT and graphene peaks. Besides the prominent SnO_2 peaks and the overlapped CNT peak, there is also a broad peak of 23°, corresponding to the (002) plane of the graphene [18]. No other peaks indicate the absence of impurities or residual SiO_2.

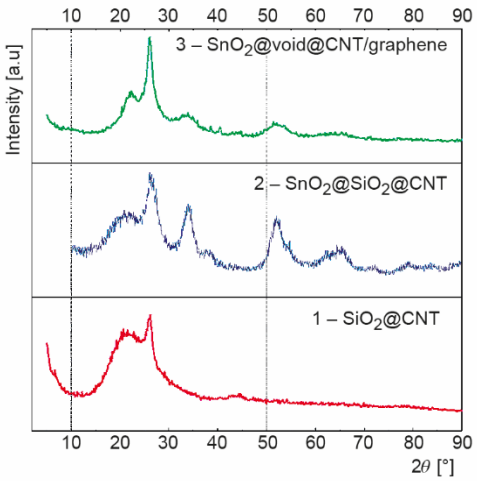

Figure 3. The XRD patterns of 1 – SiO_2@CNT, 2 – SnO_2@SiO_2@CNT and 3 – SnO_2@void@CNT/graphene

To compare the performance of SnO_2@void@CNT/graphene composite electrodes, two more types of electrodes were produced. The first is pure SnO_2 powders, SEM image and XRD pattern of which are given in fig. S4. The second one is the SnO_2/CNT/graphene electrode, which was produced as a free standing and flexible electrode by vacuum filtration method after bringing together the SnO_2 with graphene and CNT with ultrasonic processor. Figure 4(a) presents cross-sectional SEM image of SnO_2@void@CNT/graphene composite electrode. As can be seen from the image, SnO_2@void@CNT was distributed between graphene layers. Figure 4(b) displays cross-sectional SEM image of SnO_2/CNT/graphene and proves that the SnO_2 structure is placed homogeneously between the graphene sheets and the CNT. In addition to the cross-sectional images, EDS analyzes were also performed to show the SnO_2 present in the structure, figs. 4(d) and 4(e).

Figure 4(c) presents optical image of the electrodes. The free-standing electrodes were smoothly peeled off the membrane after drying at the oven. The electrodes with an average thickness of 40 μm can be easily bent like a piece of paper without any damage. In order to find the weight percentage of the SnO_2 for two electrodes, TG analyses were carried out, fig. 4(e). The weight losses before 200 °C are due to adsorbed water molecules or other small molecules. The sharp decrease in the range of 200 °C-650 °C can be explained as the combustion of carbon [27]. The SnO_2 content of the electrodes was calculated based on the mass

losses in this 200-650 °C range and determined to be 34% and 29% for SnO_2/CNT/graphene and SnO_2@void@CNT/graphene electrodes, respectively.

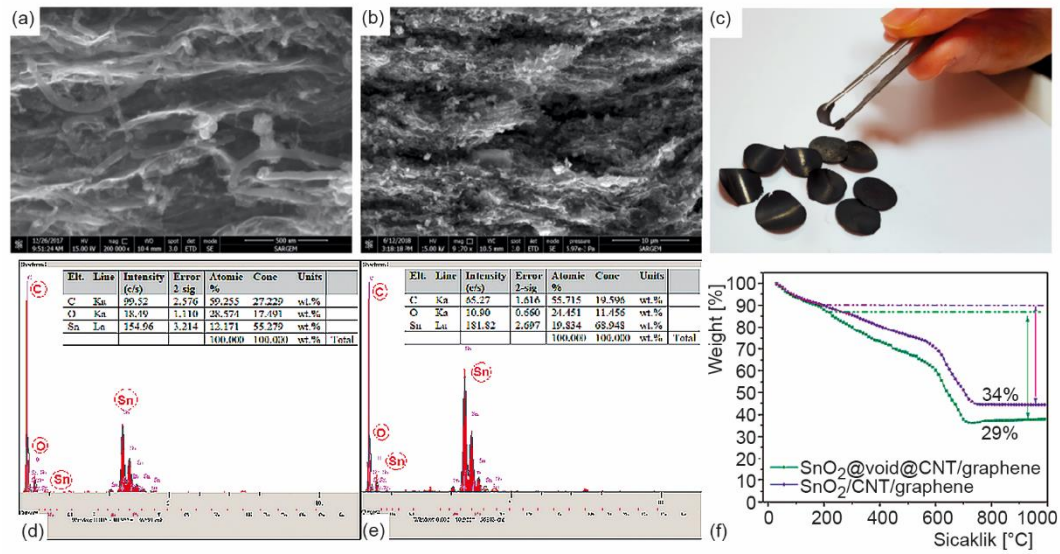

Figure 4. Cross-sectional SEM image of (a) SnO_2@void@CNT/graphene, (b) SnO_2/CNT/graphene, (c) photograph of the electrodes, EDS spectrum of (d) SnO_2@void@CNT/graphene, (e) SnO_2/CNT/graphene, and (f) TG results of the electrodes

The electrochemical properties of the SnO_2@void@CNT/graphene composite, which was produced as a solution to the problem that SnO_2 suffers as an anode material, were investigated by preparing a coin-type battery. Free-standing SnO_2@void@CNT/graphene composite electrode was directly used as a working electrode without any conductive additives or binder. Figure 5(a) presents cyclic voltammetry (CV) curves for initial five cycles between 0.01 V-3 V (*vs.* Li/Li^+). A reduction peak is observed in the first cycle at 0.57 V, indicating the formation of solid electrolyte interface (SEI) layer, eq. (1) as well as decomposition of SnO_2 to amorphous Li_2O and metallic Sn, eq. (2) [28]. In the first cathodic scan, the peak at 0.57 V is ascribed to the formation of $Li_\chi Sn$, eq. (3) [29]. The peak of this reaction is seen at 0.63 V for subsequent cycles. The slope of 0.01-0.28 can be attributed to $Li_\chi C$ formed by the induced of Li into the carbon, eq. (3) [30]. An oxidation peak is observed at 2.4 V, indicating a partially reversible Sn to SnO_2 reaction [31].

$$4Li + e^- + \text{electrolyte} \rightarrow \text{SEI (Li)} \tag{1}$$

$$SnO_2 + 4Li^+ + 4e^- \rightarrow Sn + 2Li_2O \tag{2}$$

$$Sn + \chi Li^+ + \chi e^- \leftrightarrow Li_\chi Sn\ (0 \le \chi \le 4.4) \tag{3}$$

$$C + \chi Li^+ + \chi e^- \leftrightarrow Li_\chi C \tag{4}$$

Figure 5(b) indicates charge/discharge profiles of free-standing SnO_2@void@CNT//graphene composite electrode on the selected cycles. The voltage plateaus detected in the charge and discharge curves agreeing to the oxidation/reduction peaks in the CV curves can be attributed to lithium ion insertion and de-insertion reactions. The SnO_2@void@CNT/graphene composite electrode shows specific capacity of 1197 mAh/g and 860 mAh/g for first discharge and charge, respectively. At the second cycle, the electrode exhibited 902 mAh/g and 777 mAh/g of discharge and charge capacity values. The loss of capacity after the first cycle is due to SEI film formation and damage of the structure suffering volumetric expansion [32]. Besides, coulomb efficiencies of the electrode are 71%, 86%, 97%, 96%, and 93% for 1st, 2nd, 5th, 100th, and 400th cycles, respectively.

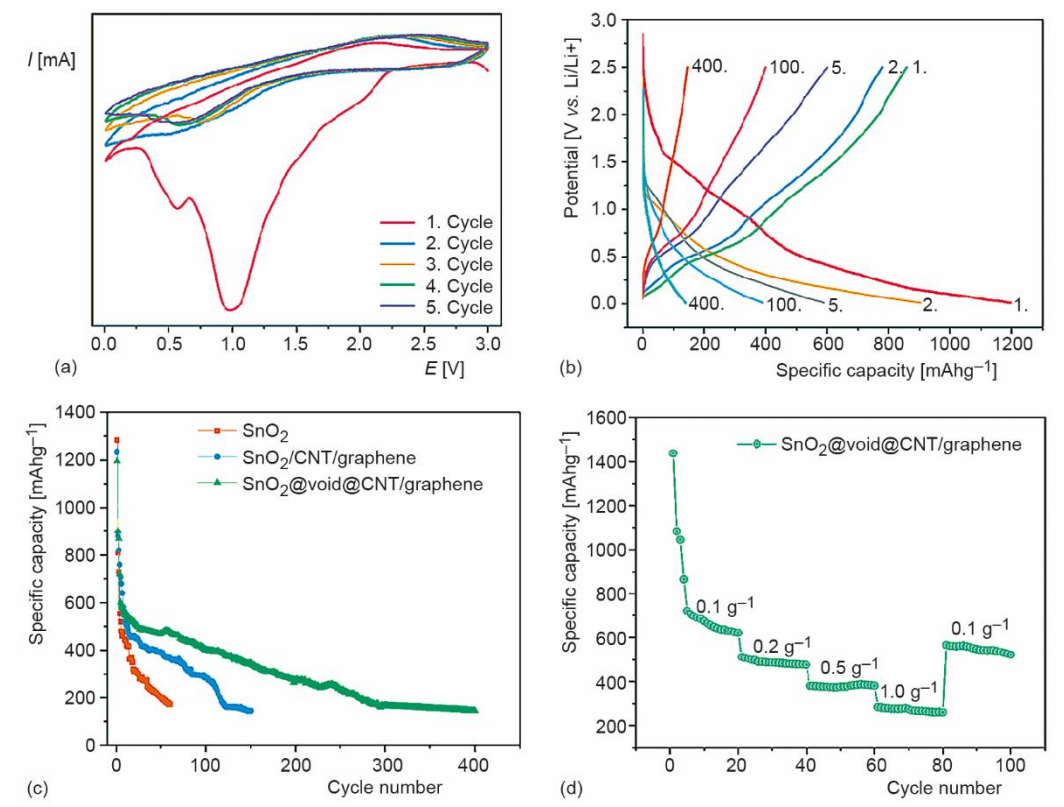

Figure 5. (a) The CV curves, (b) charge/discharge profiles of SnO_2@void@CNT/graphene electrode, (c) cycling performance of three electrodes, and (d) rate capabilities of SnO_2@void@CNT/graphene electrode

To compare the electrochemical performance of the SnO_2@void@CNT/graphene electrode, two different types of anodes were produced. An electrode was prepared with the traditional slurry method onto copper foil from pure SnO_2 powders. In addition, a free-standing and flexible electrode was made from pure SnO_2 powder, graphene and CNT named as SnO_2/CNT/graphene. Figure 5(c) presents the cycling performance of SnO_2@void@CNT/ /graphene, SnO_2/CNT/graphene and SnO_2 electrodes. The SnO_2 electrode shows the highest specific discharge capacity but after second cycle a sudden decrease is observed in capacity val-

ues. The rapid capacity drop in the first cycles is due to the formation of Li_2O and SEI on the electrode surface [33]. At the 60^{th} cycle, the battery has reached the end of its life. The drastic volume expansion that occurred during the insertion/extraction of the lithium ions caused the electrode to pulverization and made it unusable. As a solution to the problem that SnO_2 suffers as an anode material, SnO_2 powder is placed in a skeleton consisting of graphene and CNT. The SnO_2/CNT/graphene electrode exhibited a relatively stable state up to 100 cycles, although a decrease in the capacitance value was observed in the first 20 cycles. The CNT/graphene skeleton structure showed a buffering effect against volume expansion of SnO_2. Volume expansion is not the only problem with SnO_2 during alloying/dealloying process. Besides, SnO_2 particles tend to aggregate into severe Sn clusters during cycling [34]. In the SnO_2/CNT/graphene electrode, combining graphene, CNT, and SnO_2 separately may not have fully achieved the uniform distribution of SnO_2 and did not help overcome the agglomeration problem. The SnO_2@void@CNT/graphene electrode performed the best cycling performance because solutions with different perspectives have been provided to the problems that SnO_2 suffers. The SnO_2 nanotube with CNT core structure can alleviate huge volume expansion by providing void space [35]. In addition, since the structure is sandwiched between graphene layers, it is supported by a carbon-based structure both from the inside and the top. Moreover, homogeneous and nanostructured SnO_2 nucleated on CNT can shortens the diffusion distance during the cycle and prevents aggregation and pulverization [13, 36, 37]. The SnO_2@void@CNT/graphene electrode also showed remarkable rate performance in the afterwards rate test. The discharge capacities were about 400 mAh/g and 300 mAh/g when discharged at 0.5 1/Ag and 1.0 1/Ag, respectively. This performance under high current density can be attributed to fast load transfer and stable structure [38]. The electrode still shows capacity of 600 mAh/g after 100 cycles.

Conclusion

In summary, graphene layers were decorated with SnO_2 nanotube with CNT core structure (SnO_2@void@CNT) and prepared free-standing and flexible anodes for Li-ion batteries. According to structural and morphological test results, creating a void space between CNT and SnO_2 by using sacrificial SiO_2 layer, homogeneously covering the surface with SnO_2, and decoration between graphene layers were successfully carried out. In addition to this electrode, two more electrodes, pure SnO_2 and SnO_2/CNT/graphene, were produced their electrochemical properties were compared. The solution proposals applied to improve the disadvantageous electrochemical performance of SnO_2 show themselves in the battery test results. The SnO_2@void@CNT/graphene electrode exhibited a significant performance improvement in terms of capacity and rate capability.

Acknowledgment

This work is supported by the Scientific and Technological Research Council of Turkey (TUBITAK) under contract number 116M997 and Bilecik Seyh Edebali University, Coordination of Scientific Research Project under contract number 2017-01.BŞEÜ.03-01.

Electronic supplementary information

Graphene oxide production

In this study, the modified Hummer method was used for the production of graphene oxide. As a starting material, 3 g of graphite flakes were mixed in 112.5 mL H_2SO_4 and 37.5 mL HNO_3 solution for 2 hours, then washed with distilled water and dried. Then, 1 g of

graphite was subjected to heat treatment at 800 °C for 120 seconds. The thermally treated graphite was then stirred in 0.5 g of $NaNO_3$ and 23 mL of H_2SO_4 for about two hours. The beaker was placed in an ice bath, the temperature of which could be reduced to –20 °C. The 3 g of $KMnO_4$ was added carefully and mixing was continued for 30 minutes. It was then stirred at room temperature for 30 minutes. Distilled water was added to the mixture and the temperature was brought to 98 °C, and mixing was continued here. The 150 mL of distilled water and 3% H_2O_2 are added and mixed for another 2 hours and the mixture turns green. The solution obtained will be washed with 100 mL of 30% HCl solution per gram after filtering. Afterwards, it was washed with distilled water until the pH was 6-6.5 and filtered. The product obtained is called graphene oxide. Figure S1 shows XRD patterns of flake graphite and graphene oxide. Figure S2 displays Raman spectrum of graphene oxide and graphene/CNT. Figure S3 presents SEM image of bare CNT, flake graphite and graphene oxide.

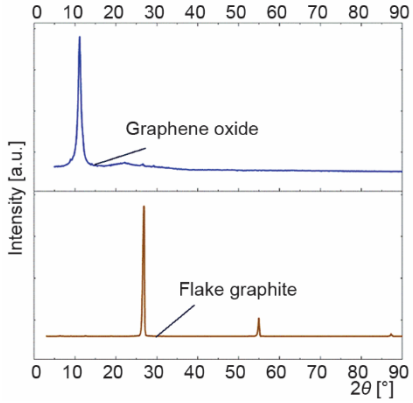

Figure S1. The XRD patterns of flake graphite and graphene oxide

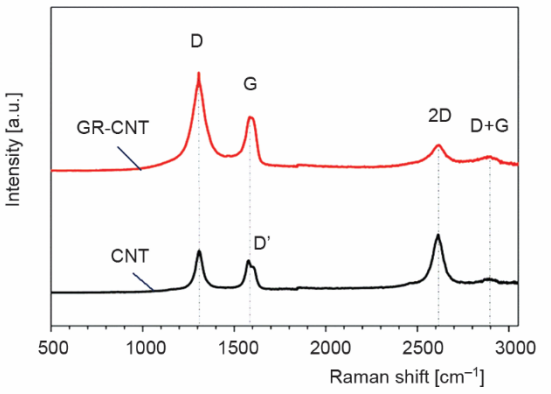

Figure S2. Raman spectrum of graphene oxide and graphene/CNT

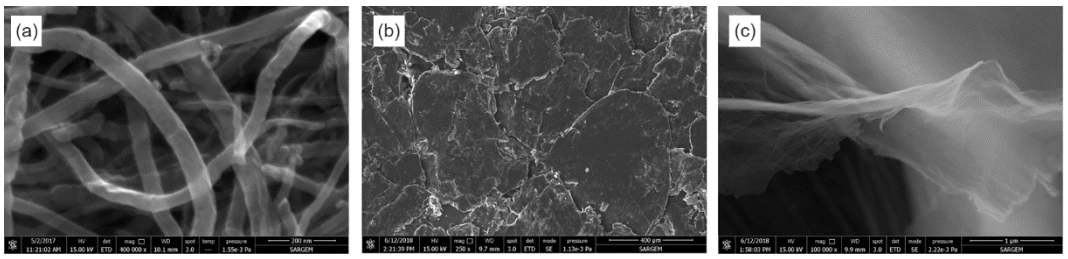

Figure S3. The SEM image of (a) bare CNT, (b) flake graphite and (c) graphene oxide

Production of oure SnO_2

The 2.25 g $SnCl_2$ and 100 mL distilled water were mixed using a magnetic stirrer for 0.5 hours. Then, the NaOH solution was slowly added into the solution until the pH value reached 13 in order to make a white precipitation and continuously stirred for another 0.5 hours. Resulting white product was washed several times in a centrifuge and dried at 80 °C for 24 hours. Figure S4 shows SEM image of SnO_2 and XRD pattern of SnO_2.

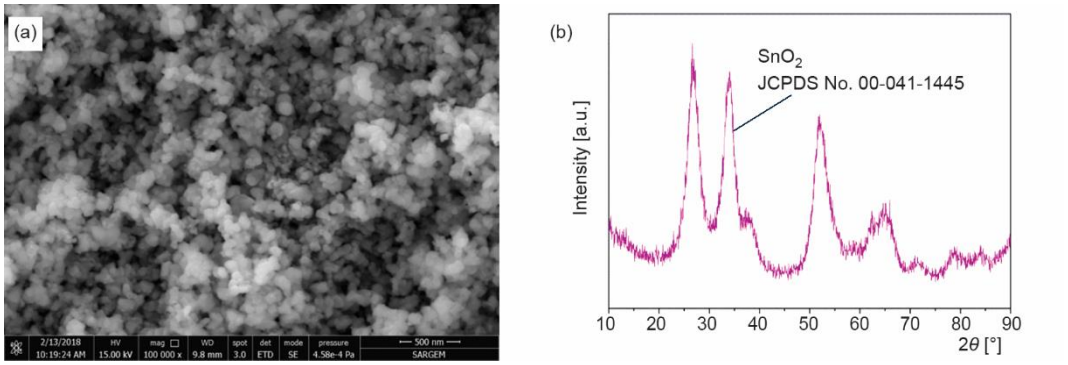

Figure S4. (a) The SEM image and (b) XRD pattern of SnO_2

Production of SnO_2 and SnO_2/CNT/graphene electrodes

Pure SnO_2 electrode was prepared by the traditional slurry method. The SnO_2 powders were added to the slurry in a weight ratio of 80% as active material. By adding 10% conductive material (carbon black) and 10% binder (PVDF dissolved in NMP solution), it was plastered on the copper foil with the dr blade technique.

To prepare SnO_2/CNT/graphene electrode, graphene oxide and CNT were dispersed in 100 mL distilled water by using ultrasonic probe. The CTAB as a surfactant was added to solution. After 30 minutes of sonication, SnO_2 powders were added and ultrasonically treated for additional 15 minutes. Then 5 mL hydrazine hydrate solution was directly added to reduce graphene oxide to graphene and sonication was carried on for an additional 15 minutes. The mixture was then vacuum filtered using PTFE filter paper (Millipore) and peeled off after drying.

References

[1] Wen, Y., *et al.*, Heteroatom-Doped Graphene for Electrochemical Energy Storage, *Chinese Sci. Bull.*, *59*, (2014), 18, pp. 2102-2121
[2] Li, Z., *et al.*, Particulate Modification of Lithium-Ion Battery Anode Materials and Electrolytes, *Particuology*, *83*, (2023), Dec., pp. 129-141
[3] Mand Khan, B., *et al.*, Role of Graphene-Based Nanocomposites as Anode Material for Lithium-Ion Batteries, *Mater. Sci. Eng. B Solid-State Mater. Adv. Technol.*, *287* (2021), Sept., 116141
[4] Ullah, K., *et al.*, Recent Trends in Graphene Based Transition Metal Oxides as Anode Materials for Rechargeable Lithium-Ion Batteries, *Nano Trends*, *1* (2022), Nov., 100004
[5] Nzereogu, P. U., *et al.*, Anode Materials for Lithium-Ion Batteries: A Review, *Appl. Surf. Sci. Adv.*, *9* (2022), Mar., 100233
[6] Yuan, S., *et al.*, Carbon-Based Materials as Anode Materials for Lithium-Ion Batteries and Lithium-Ion Capacitors: A Review, *J. Energy Storage*, *61* (2022), Dec., 106716
[7] Li, X., *et al.*, Recent Progress in the Carbon-Based Frameworks for High Specific Capacity Anodes/Cathode in Lithium/Sodium Ion Batteries, *Xinxing Tan Cailiao/New Carbon Mater.*, *36* (2021), 1, pp. 106-116
[8] Deng, X., *et al.*, SnO_2-MoO_3 Nanoparticles Anchored in Carbon Nanotubes as a Large-Capacity, High-Rate, and Long-Lifetime Anode for Lithium-Ion Batteries, *Ceram. Int.*, *47* (2021), 19, pp. 27022-27031
[9] Li, Y., *et al.*, A Nanoscale Interlayer Void Design Enabling High-Performance SnO_2-Carbon Anodes, *Carbon N. Y.*, *183* (2021), Oct., pp. 486-494
[10] Fan, B., *et al.*, A Facile Strategy Towards High Capacity and Stable Sn Anodes for Li-Ion Battery: Dual-Confinement via Sn@SnO_2 Core-Shell Nanoparticles Embedded in 3D Graphitized Porous Carbon Network, *J. Alloys Compd.*, *857* (2021), Mar., 157920

[11] Wang, X., *et al.*, Electrospun Layers by Layers Orderly Stacked SnO_2@aligned Carbon Nanofibers as High Conductivity, Long Cycle Life Self-Standing Anode for Reversible Lithium Ions Batteries, *Surfaces and Interfaces*, *29* (2022), Feb., 101814
[12] Premasudha, M., *et al.*, Hydrothermal Synthesis and Electrochemical Behaviour of SnO2/C@rGO as an Anode Material for Na-Ion Batteries, *Chem. Phys. Lett.*, *805* (2022), Feb., 139970
[13] Wei, L., *et al.*, A Facile Assembly of SnO_2 Nanoparticles and Moderately Exfoliated Graphite for Advanced Lithium-Ion Battery Anode, *Electrochim. Acta*, *432* (2022), June, 141210
[14] Wei, L., *et al.*, SnO_2/Sn Particles Anchored in Moderately Exfoliated Graphite as the Anode of Lithium-Ion Battery, *Electrochim. Acta*, *442* (2022), Dec., 141908
[15] Yang, L., *et al.*, SnO_2 Nanoparticles Composited with Biomass N-Doped Carbon Microspheres as Low Cost, Environmentally Friendly and High-Performance Anode Material for Sodium-Ion and Lithium-Ion Batteries, *J. Power Sources*, *547* (2022), Sept., pp. 1-11
[16] Xin, Y., *et al.*, Engineering Amorphous SnO_2 Nanoparticles Integrated Into Porous N-Doped Carbon Matrix as High-Performance Anode for Lithium-Ion Batteries, *J. Colloid Interface Sci.*, *639* (2023), June, pp. 133-144
[17] Li, W. L., *et al.*, Heterojunction of SnO_2/Sn Nanoparticles Coated by Graphene-Like Porous Carbon as Ultrahigh Capacity Anode of Lithium-Ion Batteries, *J. Alloys Compd.*, *948* (2023), July, 169811
[18] Zhou, F. Y., *et al.*, Porous SnO_2 Nanospheres Coated with Reduced Graphene Oxide for Formaldehyde Gas Sensor: Synthesis, Performance and Mechanism, *J. Mater. Res.*, *38* (2023), Jan., pp. 1266-1281
[19] Marcano, D. C., *et al.*, Improved Synthesis of Graphene Oxide, *ACS Nano*, *4* (2010), 8, pp. 4806-4814
[20] Alaf, M., *et al.*, Graphene Supported Heterogeneous Catalysts for Li-O_2 Batteries, *Appl. Surf. Sci.*, *380* (2016), Sept., pp. 185-192
[21] Zhang, M., *et al.*, Fabrication of Mesoporous Silica-Coated CNT and Application in Size-Selective Protein Separation, *J. Mater. Chem.*, *20* (2010), 28, pp. 5835-5842
[22] Alaf, M.,*et al.*, Double Phase Tinoxide/tin/MWCNT Nanocomposite Negative Electrodes for Lithium Microbatteries, *Microelectron. Eng.*, *126* (2014), Aug., pp. 143-147
[23] Akbulut, H., *et al.*, The Superior Surface Discharge Capacity of Core-Shell Tinoxide/Multi Walled Carbon Nanotube Nanocomposite Anodes for Li-Ion Batteries, *Acta Phys. Pol. A*, *125* (2014), 2, pp. 335-337
[24] Zhang, J. Wang, X., Microwave Absorbing Property and Preparation of CoNi@SiO2@PPy Composite in X-Band, *J. Mater. Sci. Mater. Electron.*, *29* (2018), 2, pp. 1592-1599
[25] Liang, Y., *et al.*, Synthesis and Characterization of Core-Shell Structured SiO 2 @YVO 4 :Yb 3+ ,Er 3+ Microspheres, *Appl. Surf. Sci.*, *258* (2012), 8, pp. 3689-3694
[26] Alaf, M., Akbulut, H., Electrochemical Energy Storage Behavior of Sn/SnO_2 Double Phase Nanocomposite Anodes Produced on the Multiwalled Carbon Nanotube Buckypapers for Lithium-Ion Batteries, *J. Power Sources*, *247* (2014), Feb., pp. 692-702
[27] Zhou, S., *et al.*, SnO_2 Anchored in S and N Co-Doped Carbon as the Anode for Long-Life Lithium-Ion Batteries, *Nanomaterials*, *12* (2022), 4, 700
[28] Li, H., *et al.*, Porous SNO_2hollow Microspheres as Anodes for High-Performance Lithium Ion Battery, *Mater. Lett.*, *217* (2018), Apr., pp. 276-280
[29] Liu, M., *et al.*, Octahedral Tin Dioxide Nanocrystals Anchored on Vertically Aligned Carbon Aerogels as High Capacity Anode Materials for Lithium-Ion Batteries, *Nat. Publ. Gr.*, *6* (2016), Aug., 31496
[30] Zhang, D., *et al.*, One-Step Synthesis of SnO_2/carbon Nanotube Nanonests Composites by Direct Current Arc-Discharge Plasma and Its Application in Lithium-Ion Batteries, *Nanomaterials*, *11* (2021), 11, 3138
[31] Jiang, S., *et al.*, Free-Standing SnO_2@rGO Anode via the Anti-solvent-assisted Precipitation for Superior Lithium Storage Performance, *Front. Chem.*, *7* (2019), Dec., pp. 1-10
[32] Ma, D., *et al.*, Novel Hollow SnO_2 Nanosphere @ TiO 2 Yolk - Shell Hierarchical Nano- Spheres as Anode Material for High-Performance Lithium-Ion Batteries, *Mater. Lett.*, *157* (2015), Oct., pp. 228-230
[33] Zhang, B., *et al.*, SnO_2-Graphene-Carbon Nanotube Mixture for Anode Material with Improved Rate Capacities, *Carbon N. Y.*, *49* (2011), 13, pp. 4524-4534
[34] Kebede, M. A., Tin Oxide-Based Anodes for Both Lithium-Ion and Sodium-Ion Batteries, *Curr. Opin. Electrochem.*, *21* (2020), 1, pp. 182-187
[35] Li, B., *et al.*, Yolk-Shelled SnO_2@NxC Spheres with Controllable Void Space as High-Capacity and Cycle-Stable Anode Materials for Lithium-Ion Batteries, *Mater. Des.*, *219* (2022), July, 110745

[36] Zhou, D., *et al.*, Three-Dimensional Porous Graphene-Encapsulated CNT@SnO_2composite for High-Performance Lithium and Sodium Storage, *Electrochim. Acta*, *230* (2017), Mar., pp. 212-221
[37] Dhanabalan, A., *et al.*, Porous SnO_2/CNT Composite Anodes: Influence of Composition and Deposition Temperature on the Electrochemical Performance, *J. Mater. Res.*, *25* (2010), 8, pp. 1554-1560
[38] Zhu, S., *et al.*, Precise Growth of Al_2O_3/SnO_2/CNT Composites by a Two-Step Atomic Layer Deposition and Their Application as an Improved Anode for Lithium Ion Batteries, *Electrochim. Acta*, *319* (2019), Oct., pp. 490-498

Paper submitted: November 18, 2022
Paper revised: November 30, 2022
Paper accepted: May 13, 2023